PCCP

Differentiation of Peptide Isomers by Excited-State Photodissociation and Ion-Molecule Interactions

Journal:	*Physical Chemistry Chemical Physics*
Manuscript ID	CP-ART-08-2020-004111.R1
Article Type:	Paper
Date Submitted by the Author:	22-Sep-2020
Complete List of Authors:	Van Orman, Brielle; UC Riverside Wu, Hoi-Ting; UC Riverside, Chemistry Julian, Ryan; UC Riverside,

Differentiation of Peptide Isomers by Excited-State Photodissociation and Ion-Molecule Interactions

Brielle L. Van Orman, Hoi-Ting Wu, Ryan R. Julian*

Department of Chemistry, University of California, Riverside, California 92521, United States

*corresponding author: ryan.julian@ucr.edu

Abstract

Solvochromatic effects are most frequently associated with solution-phase phenomena. However, in the gas phase, the absence of solvent leads to intramolecular solvation that can be driven by strong forces including hydrogen bonds and ion-dipole interactions. Here we examine whether isomerization of a single residue in a peptide results in structural changes sufficient to shift the absorption of light by an appended chromophore. By carrying out the experiments inside a mass spectrometer, we can easily monitor photodissociation yield as a readout for chromophore excitation. A series of peptides of different lengths, charge states, and position and identity of the isomerized residue were examined by excitation with both 266 and 213 nm light. The results reveal that differences in intramolecular solvation do lead to solvochromatic shifts in many cases. In addition, the primary product following photoexcitation is a radical. Ion-molecule reactions with this radical and adventitious oxygen were monitored and also found to vary as a function of isomeric state. In this case, differences in intramolecular solvation alter the availability of the reactive radical. Overall, the results reveal that small changes in a single amino acid can influence the overall structural ensemble sufficient to alter the efficiency of multiple gas-phase reactions.

Introduction

Absorption of a particular wavelength of light in molecules is primarily dictated by the proper organization of electrons within chemical bonds to form a suitable chromophore. However, absorption can also be influenced by the environment surrounding a chromophore (as shown in Scheme 1). For example, the maxima at which the same chromophore can absorb or emit can shift if the solvent is changed. Such solvochromatic effects are complex,[1] but they fundamentally derive from differences in the polarity of solvents and how solvent molecules interact with the chromophore. In the context of larger molecules such as proteins, solvation of the chromophore can be achieved either partially or entirely by the molecule itself. This allows intrinsic chromophores such as tryptophan to be used as sensitive probes of protein structure.[2] Structural changes due to modulation of external factors such as pH or temperature can be detected if they influence the local hydrogen bonding, salt bridges, or hydrophobic pockets surrounding the tryptophan sidechain. This approach has been further extended by the development and use of extrinsic dyes that can be appended to specific sites and tailored to provide information about highly complex protein systems.[3] These examples make it clear that chromophoric absorption of light can be a powerful structural tool, one that is potentially sensitive to minor changes in environment.

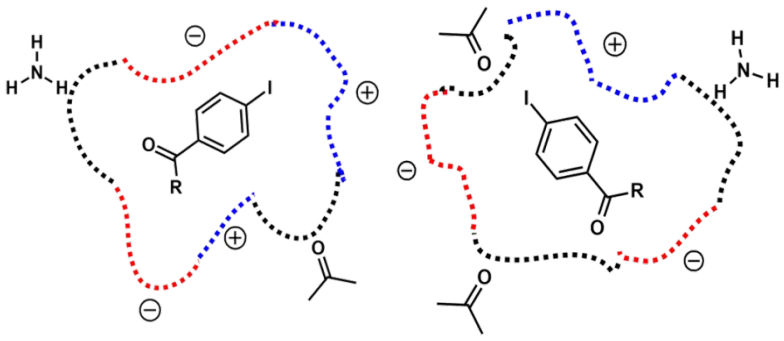

Scheme 1. Different solvation environments created by alternate arrangements of charged and polar groups could potentially influence the photochemistry of an active chromophore.

Indeed, recent work has demonstrated that solvatochromism can be used to distinguish similar compounds, including isomers.[4] Isomers and their significance are often overlooked. Isomers are very important in biology, for example, spontaneous isomerization of amino acids within long-lived proteins is known to occur by several mechanisms.[5-7] Isomerization within these proteins can prevent their degradation, which may be important in several age-related diseases including Alzheimer's disease and cataracts.[8-10] Due to the nature of isomers, they are inherently difficult to differentiate. Isomers within non-biological materials can have effects on physical properties as well. For example, isomers of tetrathienoanthracene have been found to have different optical and electrochemical properties, as well as differing thermodynamic stabilities of radical cations.[11] In addition to materials, synthesis and differentiation of pharmaceutically relevant isomers is important. Inverted chirality in drugs can greatly reduce efficacy, and in some cases even cause harm, as demonstrated in studies on antitumor, antidepressant, and antipsychotic drugs.[12,13]

Fragmentation is another strategy for isomer identification and includes methods that utilize photochemistry to cleave bonds. Infrared multiphoton dissociation (IRMPD) has been used to successfully differentiate similar structures, including isomers. For example, glucose disaccharide linkage isomers can be identified with wavelength-tunable IRMPD-MS in combination with lithium tags because fragment ion abundance at specific wavelengths differs between isomers.[14] Small changes in structure have been differentiated by combining IR and ultraviolet (UV) excitation to analyze cold H_2O^+-benzo crown ether complexes.[15] In this system, IR-UV spectra in the region of C-H and O-H stretches are compared. Another study using UVPD to generate a radical, followed by addition of collisional energy to yield radical-directed dissociation (RDD) reported the ability to differentiate glycan isomers.[16] UVPD has also proven useful in the characterization of protein conformers related to cis/tran isomerization at proline.[17] Excited state chemistry involving photo-detachment of electrons has recently enabled circular

dichroism-like characterization of DNA strands in the gas phase.[18] Structural information can also be obtained by action spectroscopy, which has revealed structural differences in sequence mutants of amyloid-beta.[19]

In the current study, peptides were tagged with *para*-iodobenzoic acid (4IB) to determine whether small structural changes such as isomerized residues would sufficiently influence chromophore excitation and subsequent fragmentation to allow isomer identification. Peptides containing aspartic acid (Asp), glutamic acid (Glu), and serine (Ser) isomers were subjected to UVPD at 213 nm and 266 nm. Photoexcitation of 4IB leads primarily to loss of iodine following excited state dissociation of the carbon–iodine bond for all isomers, but the relative fragment-ion intensity was found to be sensitive to isomeric form for some peptides. Molecular dynamics calculations reveal that isomers adopt different structural ensembles in the gas phase, which alters solvation and absorption of UV photons by 4IB.

Methods

Peptide synthesis. The peptides AIPVSR (L-Ser and D-Ser forms), VKLDHG (L-Asp, D-Asp, L-isoAsp, D-isoAsp), VKLDSG (L-Asp, D-Asp, L-isoAsp, D-isoAsp), VHLGGEGYK (L-isoGlu, D-isoGlu), and VTIHEGGPWFK (L-Glu, D-isoGlu) were synthesized as previously described and tagged on bead with *para*-iodobenzoic acid (4IB) on the N-terminus in order to create a photocleavable bond for radical formation.[20]

UVPD experiments. UVPD experiments at 213 nm were conducted using an Orbitrap Velos Pro with an HCD (higher-energy collisional dissociation) cell modified with a quartz window to accept pulses from a 213 nm FQSS 213-Q4 laser. Photoactivation was carried out by inserting ions without collisional excitation and trapping them for 300 ms with the laser firing at 1000 Hz rep rate. UVPD experiments at 266 nm were performed in an LTQ ion trap mass spectrometer (Thermo Fisher Scientific, San Jose, CA). The ion trap was modified to accommodate an Nd:YAG laser (Continuum, Santa Clara, CA) with a quartz window at the back of the ion trap.

Data. In order to evaluate chromophore excitation, data points were first sorted by intensity and the lowest ten intensities were eliminated to omit blank scans. The intensity of the loss of iodine was then plotted against the total ion count and fit with a linear regression. The slope and error of the fit were used to determine the relative abundance and standard deviation. To evaluate ion-molecule interactions in the 213 nm experiments, intensities of oxygen adducts were treated identically to loss of iodine.

Simulated Annealing. To find structural differences between the peptide isomers of 4IB-VKLDHG, simulated annealing was performed using MacroModel (Schrödinger Inc., Portland, Oregon). Using the OPLS2005 force field, structures were heated to 1000 K and cooled to 200 K, followed by minimization. The outputs from 1000 rounds of annealing were collected, sorted by potential energy, and the structures within 50 kJ of the lowest energy structure were retained. Maestro (Schrödinger Inc., Portland, Oregon) was used to extract distances between pairs of atoms for structural comparisons as described below.

Results and Discussion

To evaluate whether chromophore excitation in the gas phase is sensitive to changes in molecular structure arising from isomerization, we conducted UVPD experiments on a series of peptide isomers. In lieu of monitoring absorption or emission directly, the magnitude of fragmentation caused by the absorption of 266 or 213 nm light was monitored with mass spectrometry. Chromophores containing carbon-iodine bonds that are particularly labile when excited at these wavelengths were covalently attached to each isomer in identical fashion. The primary fragment following photoactivation is loss of iodine as illustrated for L/D Asp isomers of the peptide 4IB-VKLDSG in Fig. 1. The preferential loss of iodine holds true for both excitation wavelengths, although it can be observed that 266 nm light is more selective in exciting this fragmentation pathway almost exclusively. At first glance, the fragmentation spectra obtained for each isomer appear identical, but closer inspection reveals subtle differences in the relative

intensities. For example, the abundance of the c_4 fragment varies by isomer. Furthermore, the loss of iodine relative to the precursor ion varies by isomer for excitation at 213 nm (Figs. 1a and 1b).

Subsequent to loss of iodine in Figs. 1a and 1b, ion-molecule reactions leading to addition of oxygen are noted (observed as +O and $+O_2$ adducts). These reactions occur due to the presence of trace oxygen impurities in the HCD cell that is filled with N_2 collision gas. The radical peptides formed by loss of iodine can easily react with molecular oxygen, which is also a radical, by way of recombination.[21,22] The radicals are retained in the HCD cell for 300 ms, allowing ample time for these adducts to form even at very low oxygen levels. Addition of both +16 Da and +32 Da is observed. The addition of +16 Da likely occurs sequentially when the initial addition of O_2 is followed by UVPD of the resulting peroxyl bond by a subsequent laser shot leading to loss of O.[23] In support of this possibility, the relative abundance of the +16 Da peak in comparison to the +32 Da peak increased with increasing activation time as shown in Fig. S2. The abundance of oxygen adducts also appears to be sensitive to isomeric form.

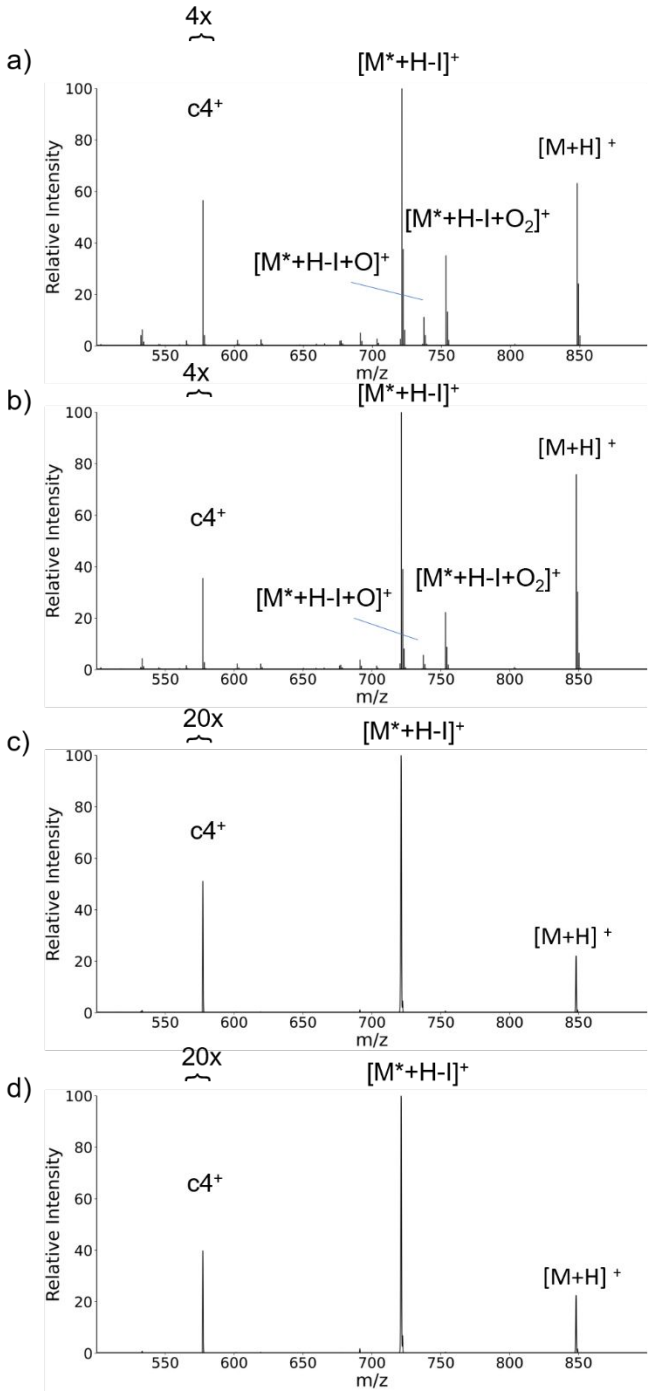

Fig 1. Representative mass spectra from isomers of 4IB-VKLDSG (underlined residue locates isomerized position) used to quantitate chromophore excitation at 213 nm a) L-Asp and b) D-Asp and at 266 nm c) L-Asp and d) D-Asp.

To facilitate quantitative comparisons, intensity data from mass spectra are presented in bar graph format as shown in Fig. 2 where the ratios of iodine loss to total ion count for peptides containing Asp isomers are shown. Numerical values for all UVPD yields are provided in Table 1. Asp isomers were selected for these experiments because they represent the most abundant site of isomerization in peptides and have been demonstrated to interfere with protein degradation in biology.[8,10,24] Excitation at both 266 nm (orange bars) and 213 nm (blue bars) was explored. The relative abundances are only relevant within each wavelength, i.e. only the orange bars should be compared to each other. Results for the singly protonated peptide [4IB-VKLDSG+H]$^+$ are shown in Fig. 2a, where excitation at 266 nm yields similar ratios for all isomers. In fact, for the 266 nm ratios, the maximum difference is 2% outside the standard deviation represented by the error bars. In contrast, 213 nm yields greater differences in loss of iodine for Asp isomers, with differences outside error ranging from 13% to 55%. Additional results for the peptide 4IB-VKLDHG are shown in Figs. 2b and 2c. Exchanging serine for histidine also allows the peptide to pick up another proton, enabling the influence of charge state to be examined. Interestingly, the L/D-Asp isomers in the +1 charge state can be differentiated from the L/D-isoAsp isomers following excitation at both 266 and 213 nm, although the magnitude of variation is not large (~3% and 52% max for 266 and 213 nm, respectively). The +2 charge state results in Fig. 2c are similar to those in Fig. 2a in that the 266 nm ratios are similar and vary less than those observed for 213 nm (although the ratios themselves are different for each peptide). Overall, the results in Fig. 2 suggest that 213 nm excitation is more sensitive to isomer structure. This may be a result of the greater number of chromophores that 213 nm light can excite,[25] which include both the benzyl group and peptide bonds. In contrast, excitation at 266 nm is primarily limited to aromatic groups (including high absorption for 4IB).[26] The greater number of chromophores at 213 nm may enhance the likelihood for interaction via energy transfer to the labile carbon–iodine bond.

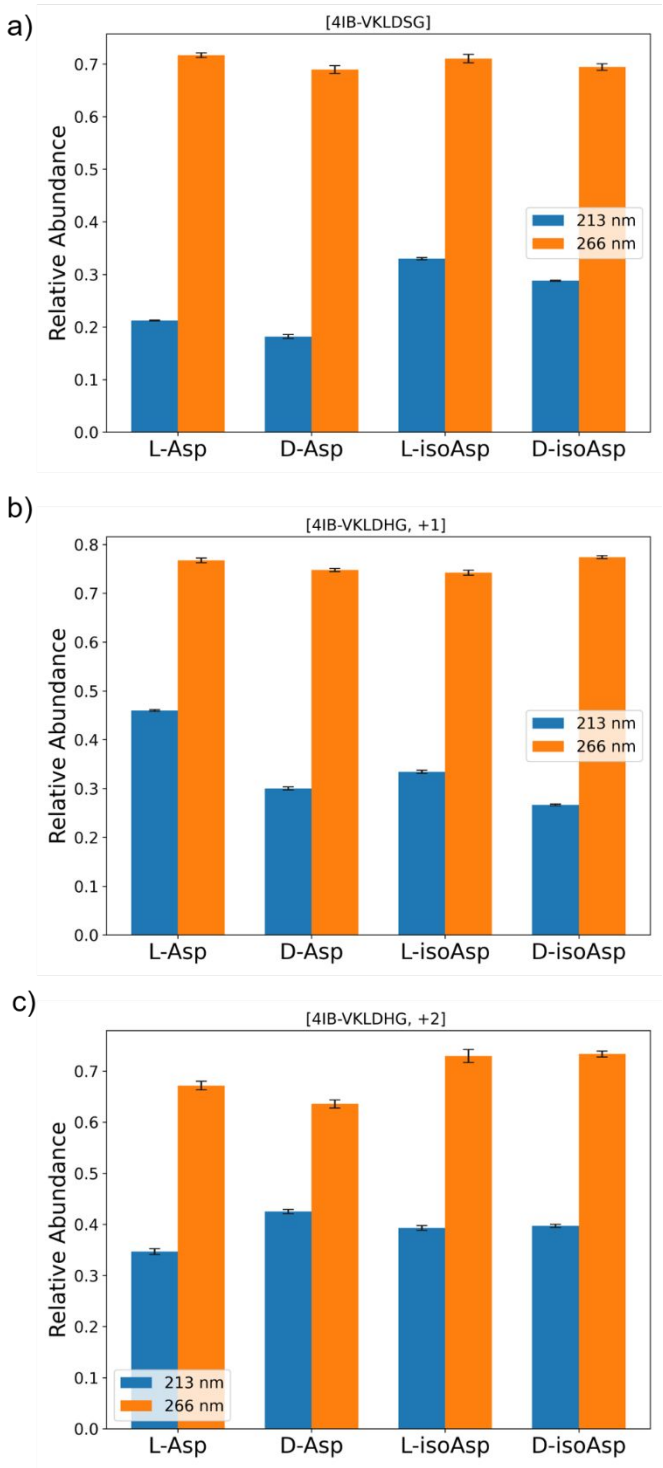

Fig. 2 Relative chromophore excitation for a) [4IB-VKLDSG+H]$^{+}$ b) [4IB-VKLDHG+H]$^{+}$ and c) [4IB-VKLDHG+H]$^{2+}$ following excitation at 213 nm (shown in blue) and 266 nm (shown in orange). Error bars represent standard error of regression.

To explore how other sites of isomerization influence peptide structure and light absorption, we examined peptides isomerized at serine and glutamic acid (4IB-AIPVSR, 4IB-VHLGGEGYK, and 4IB-VTIHEGGPWFK), which are also modification sites of biological interest as serine is the second most abundant site of isomerization and glutamic acid can mimic aspartic acid isomerization pathways. [6,27] The peptide containing serine, 4IB-AIPVSR, is easily distinguished by 213 nm excitation (40% difference) but not by 266 nm light (error bars overlap). The serine side chain is small but is capable of forming hydrogen bonds. The results suggest that the serine side chain does not form a hydrogen bond near the 4IB group (due to absence of difference at 266 nm), but may form different hydrogen bonds with backbone groups that interact with 213 nm light. Peptides with glutamic acid isomers, 4IB-VHLGGEGYK and 4IB-VTIHEGGPWFK, contain additional native chromophores in the tyrosine and tryptophan side chains. Although there are measurable differences in the intensity of the loss of iodine for both peptides, the differences are not impressive, though statistically more relevant for the data acquired at 213 nm. These peptides are also longer (with 3 and 5 additional residues beyond those discussed above), which may lead to dilution of any differences in solvatochromatic effects because a lower percentage of the peptide is represented by the isomerized site. Numerical values for the data from Figs. 2 and 3 are provided in Table 1.

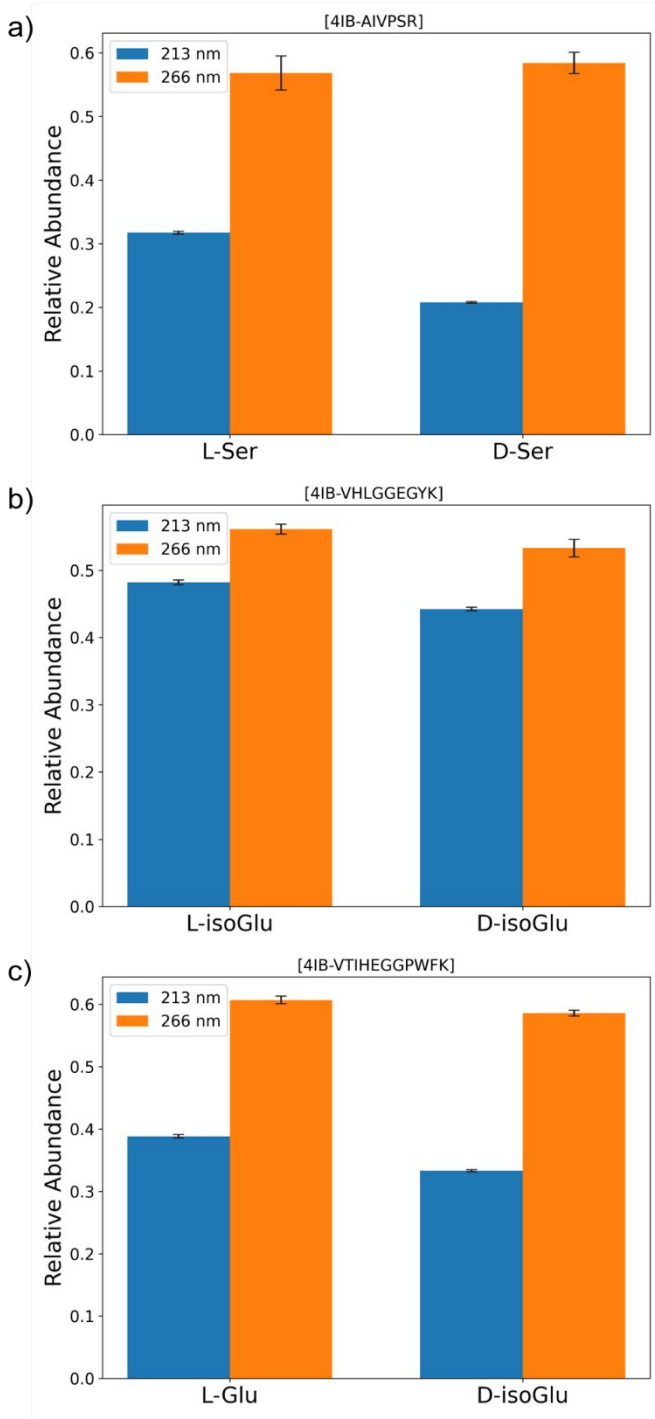

Fig. 3 Relative chromophore excitation in peptides a) [4IB-AIPVSR+H]$^+$, b) [4IB-VHLGGEGYK+H]$^+$, and c) [4IB-VTIHEGGPWFK+H]$^+$ at UVPD 213 nm (shown in blue) and 266 nm (shown in orange). Error bars represent standard error of regression.

Table 1. Numerical values for PD yields

Peptide	Isomer	Charge State	213 PD Yield	213 Error	266 PD Yield	266 Error
AIPVSR	L-Ser	+1	0.32	0.002	0.57	0.027
AIPVSR	D-Ser	+1	0.21	0.001	0.58	0.017
VKLDSG	L-Asp	+1	0.21	0.001	0.72	0.004
VKLDSG	D-Asp	+1	0.18	0.004	0.69	0.008
VKLDSG	L-isoAsp	+1	0.33	0.002	0.71	0.008
VKLDSG	D-isoAsp	+1	0.29	0.001	0.69	0.006
VKLDHG	L-Asp	+1	0.46	0.002	0.77	0.005
VKLDHG	D-Asp	+1	0.30	0.003	0.75	0.003
VKLDHG	L-isoAsp	+1	0.33	0.003	0.74	0.005
VKLDHG	D-isoAsp	+1	0.27	0.002	0.77	0.003
VKLDHG	L-Asp	+2	0.35	0.005	0.67	0.008
VKLDHG	D-Asp	+2	0.43	0.004	0.64	0.008
VKLDHG	L-isoAsp	+2	0.39	0.005	0.73	0.013
VKLDHG	D-isoAsp	+2	0.40	0.003	0.73	0.006
VHLGGEGYK	L-isoGlu	+1	0.48	0.004	0.56	0.007
VHLGGEGYK	D-isoGlu	+1	0.44	0.003	0.53	0.013
VTIHEGGPWFK	L-Glu	+1	0.39	0.003	0.61	0.006
VTIHEGGPWFK	D-isoGlu	+1	0.33	0.002	0.59	0.005

Simulations. Simulated annealing of each of the Asp isomers of 4IB-VKLDHG in the +1 charge state was carried out to explore low energy gas-phase structures and evaluate potential sources of the observed differences in photodissociation yields observed experimentally in Fig. 2b. Distances from the iodine atom of 4IB to the central carboxyl carbon of the Asp side chain are shown as a function of potential energy for all structures within 50 kJ/mol of the lowest energy conformation in Fig. 4. To the right of each scatter plot, a histogram of the distances is shown to allow quantitative comparison of the results. Both the scatter plots and histograms vary between isomers. The L-Asp peptide has isomers with distances spanning a wide range centered at ~11 Å. In contrast, D-Asp appears to favor two structural populations with distances centered at 5-6 Å and ~11 Å. Interestingly, L-isoAsp appears to favor structures with shorter 5-6 Å distances, while D-isoAsp favors structures with a unique distance of ~7-8 Å. These

simulations reveal that small changes, such as isomerization of a single residue can influence the distribution of structures and intramolecular solvation for a small chromophore such as 4IB. While it is not the intent of this project to identify the actual gas phase structure or structures for these isomeric peptides and additional simulations would be required on different charge state configurations to completely evaluate structural space, it is clear from the results in Fig. 4 that structural differences can occur as a result of single residue isomerization.

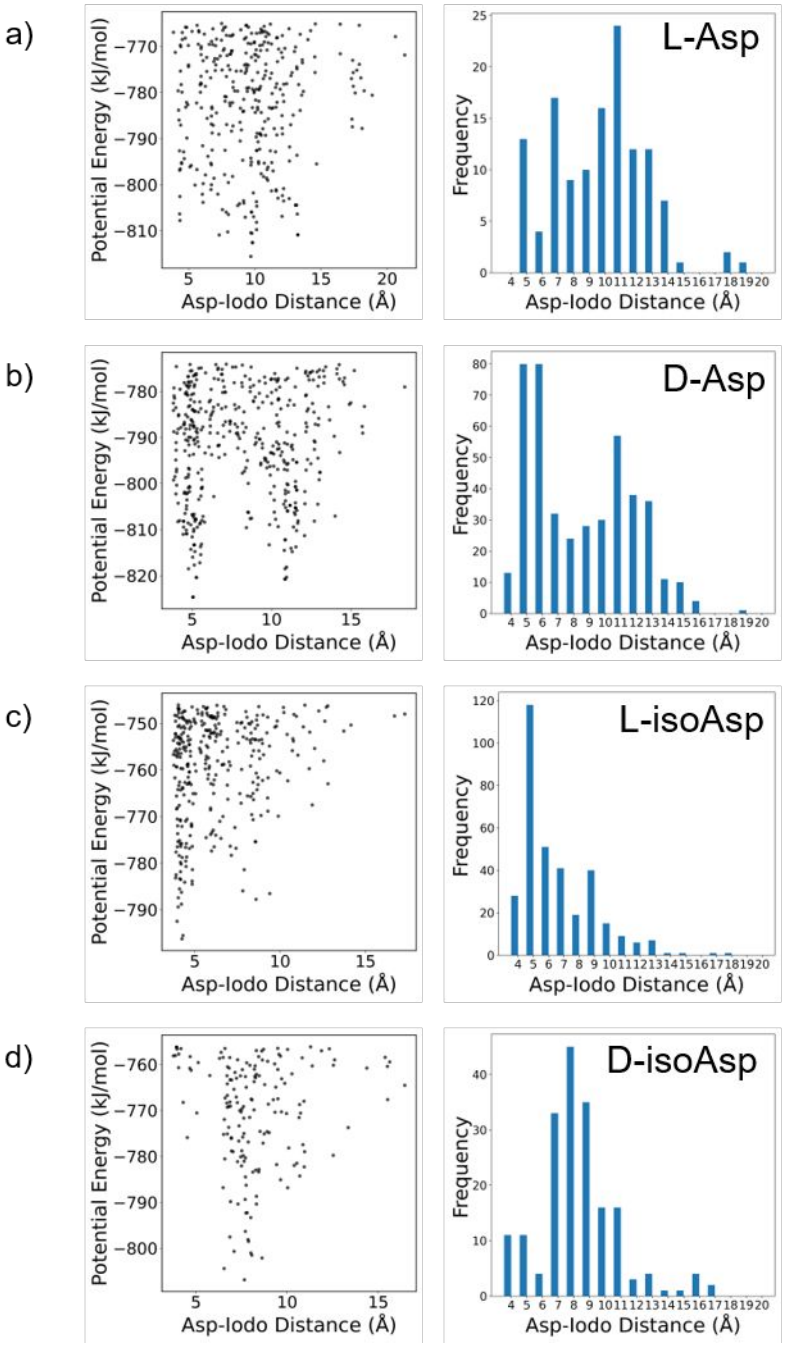

Fig. 4 Simulated annealing results for 4IB-VKLDHG protonated on lysine. Scatter plots on the left show the potential energy of structures within 50 kJ of the lowest energy structure versus the distance between the iodine atom on 4IB and the central carbon of the aspartic acid in the side chain. On the right, the number of structures within each distance bin are shown in a histogram.

Ion-molecule reactions. Ion-molecule reactions have been used for decades to examine peptide structure in the gas phase.[28-30] In particular, ion-molecule reactions between radical species and oxygen are convenient when carried out with adventitious/contaminant oxygen.[31-34] The same structural differences between isomeric peptides that influence chromophore excitation (such as solvation or absence of it) can also potentially affect the rates of ion-molecule reactions. As discussed above, trace levels of O_2 in the HCD cell lead to ion molecule reactions between the radical peptides and O_2 (see Fig. 1). The relative intensities of the +O and $+O_2$ adducts for 4IB-VKLDSG and 4IB-AIPVSR peptide isomers are shown in Fig. 5 and summarized in Table 2. Interestingly, for 4IB-AIPVSR the epimers can be distinguished by both the +O and $+O_2$ adducts. Furthermore, the ratio of the two adducts appear to be correlated with the +O adduct appearing at roughly half the intensity of the $+O_2$ adduct for both isomers. For 4IB-VKLDSG, all for isomers can be identified as well, but the intensities of the +O and $+O_2$ adducts are not correlated between isomers. The most intense and least intense adducts are not the same for the +O and $+O_2$ adducts. The results in Fig. 5 suggest that ion-molecule reactions are very sensitive to three-dimensional structure, enabling identification of isomeric form.

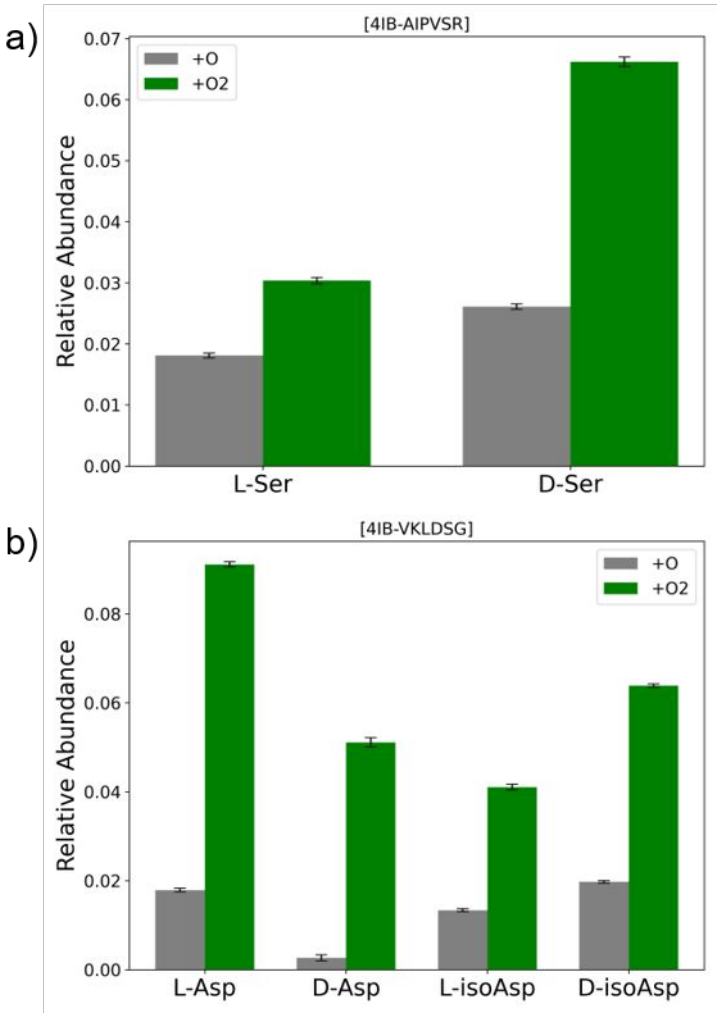

Fig 5. Formation of +O (shown in gray) and $+O_2$ (shown in green) adducts in a) [4IB-AIPVSR+H]$^+$ and b) [4IB-VKLDSG+H]$^+$. These adducts were only observed in significant abundances in 213 nm experiments. Error bars represent standard error of regression.

Table 2. Numerical values for ion-molecule oxygen adducts

Peptide	Isomer	Charge State	+16 Yield	+16 Error	+32 Yield	+16 Error
VKLDHG	L-Asp	+2	0.018	0.0004	0.091	0.0006
VKLDHG	D-Asp	+2	0.003	0.0007	0.051	0.0011
VKLDHG	L-isoAsp	+2	0.013	0.0004	0.041	0.0007
VKLDHG	D-isoAsp	+2	0.020	0.0003	0.064	0.0004

Conclusions

We have demonstrated that solvatochromic perturbations due to differences in three-dimensional structure between isomeric peptides lead to differences in the absorption of UV light. These differences can be easily quantified by examining the extent of iodine loss in peptides with carbon–iodine containing chromophores. The excitation wavelength is important, with our results suggesting that better structural sensitivity is achieved with 213 nm light. This may be attributable to excitation of additional chromophores such as peptide bonds. The results suggest that sensitivity to isomeric form is reduced as peptide size increases, implying there may be an upper limit to the size of isomer that can be identified. Ion-molecule reactions between the radicals generated by UVPD and adventitious molecular oxygen proved to be quite sensitive to isomeric form. In systems where such reactions can be carried out without modification of instrumentation, this approach may be attractive.

Acknowledgements. The authors acknowledge funding from the National Science Foundation (1904577).

References

[1] Marini, A.; Muñoz-Losa, A.; Biancardi, A.; Mennucci, B. What Is Solvatochromism? *J. Phys. Chem. B.* **2010**, *114* (51), 17128–17135.

[2] Ghisaidoobe, A.; Chung, S. Intrinsic Tryptophan Fluorescence in the Detection and Analysis of Proteins: A Focus on Förster Resonance Energy Transfer Techniques. *Int. J. Mol. Sci.* **2014**, *15* (12), 22518–22538.

[3] Loving, G. S.; Sainlos, M.; Imperiali, B. Monitoring Protein Interactions and Dynamics with Solvatochromic Fluorophores. *Trends Biotechnol.* **2010**, *28* (2), 73–83.

[4] Madeira, P. P.; Loureiro, J. A.; Freire, M. G.; Coutinho, J. A. P. Solvatochromism as a New Tool to Distinguish Structurally Similar Compounds. *J. Mol. Liq.* **2019**, *274*, 740–745.

[5] Robinson, N. E.; Robinson, Z. W.; Robinson, B. R.; Robinson, A. L.; Robinson, J. A.; Robinson, M. L.; Robinson, A. B. Structure-Dependent Nonenzymatic Deamidation of Glutaminyl and Asparaginyl Pentapeptides. *J. Pept. Res.* **2004**, *63* (5), 426–436. https://doi.org/10.1111/j.1399-3011.2004.00151.x.

[6] Riggs, D. L.; Silzel, J. W.; Lyon, Y. A.; Kang, A. S.; Julian, R. Analysis of Glutamine Deamidation: Products, Pathways, and Kinetics. *Anal. Chem*. **2019**, *91*, 13032−13038. https://doi.org/10.26434/chemrxiv.8852246.v1.

[7] Radkiewicz, J. L.; Zipse, H.; Clarke, S.; Houk, K. N. Accelerated Racemization of Aspartic Acid and Asparagine Residues via Succinimide Intermediates: An Ab Initio Theoretical Exploration of Mechanism. *J. Am. Chem. Soc.* **1996**, *118* (38), 9148–9155. https://doi.org/10.1021/ja953505b.

[8] Lambeth, T. R.; Riggs, D. L.; Talbert, L. E.; Tang, J.; Coburn, E.; Kang, A. S.; Noll, J.; Augello, C.; Ford, B. D.; Julian, R. R. Spontaneous Isomerization of Long-Lived Proteins Provides a Molecular Mechanism for the Lysosomal Failure Observed in Alzheimer's Disease. *ACS Cent. Sci.* **2019**, *5* (8), 1387–1395. https://doi.org/10.1021/acscentsci.9b00369.

[9] Lyon, Y. A.; Collier, M. P.; Riggs, D. L.; Degiacomi, M. T.; P Benesch, J. L.; Julian, R. R. Structural and Functional Consequences of Age-Related Isomerization in α-Crystallins. *J. Biol. Chem.* **2019,** *294* (19), 7546–7555. https://doi.org/10.1074/jbc.RA118.007052.

[10] Geiger, T.; Clarke, S. Deamidation, Isomerization, and Racemization at Asparaginyl and Aspartyl Residues in Peptides: Succinimide-Linked Reactions That Contribute to Protein Degradation. *J. Biol. Chem.* **1987,** *262* (2), 785-794.

[11] Brusso, J. L.; Hirst, O. D.; Dadvand, A.; Ganesan, S.; Cicoira, F.; Robertson, C. M.; Oakley, R. T.; Rosei, F.; Perepichka, D. F. Two-Dimensional Structural Motif in Thienoacene Semiconductors: Synthesis, Structure, and Properties of Tetrathienoanthracene Isomers. *Chem. Mater.* **2008**, *20* (7), 2484–2494. https://doi.org/10.1021/cm7030653.

[12] Arnesano, F.; Pannunzio, A.; Coluccia, M.; Natile, G. Effect of Chirality in Platinum Drugs. *Coordination Chemistry Reviews.* **2015**, *284,* 286–297. https://doi.org/10.1016/j.ccr.2014.07.016.

[13] Coutts, R. T.; Baker, G. B. Implications of Chirality and Geometric Isomerism in Some Psychoactive Drugs and Their Metabolites. *Chirality* **1989**, *1* (2), 99–120. https://doi.org/10.1002/chir.530010204.

[14] Polfer, N. C.; Valle, J. J.; Moore, D. T.; Oomens, J.; Eyler, J. R.; Bendiak, B. Differentiation of Isomers by Wavelength-Tunable Infrared Multiple-Photon Dissociation-Mass Spectrometry: Application to Glucose-Containing Disaccharides. *Anal. Chem.* **2006**, *78* (3), 670–679. https://doi.org/10.1021/ac0519458.

[15] Inokuchi, Y.; Ebata, T.; Rizzo, T. R. UV and IR Spectroscopy of Cold H 2 O + −Benzo-Crown Ether Complexes. *J. Chem. Phys. A* **2015**, *119,* 11113-11118. https://doi.org/10.1021/acs.jpca.5b07033.

[16] Riggs, D. L.; Hofmann, J.; Hahm, H. S.; Seeberger, P. H.; Pagel, K.; Julian, R. R. Glycan Isomer Identification Using Ultraviolet Photodissociation Initiated Radical Chemistry. *Anal. Chem.* **2018**, *90* (19), 11581–11588. https://doi.org/10.1021/acs.analchem.8b02958.

[17] Warnke, S.; von Helden, G.; Pagel, K. Analyzing the Higher Order Structure of Proteins with Conformer-Selective Ultraviolet Photodissociation. *Proteomics* **2015**, *15* (16), 2804–2812.

[18] Daly, S.; Rosu, F.; Gabelica, V. Mass-Resolved Electronic Circular Dichroism Ion Spectroscopy. *Science* **2020**, *368* (6498), 1465–1468.

[19] Daly, S.; Kulesza, A.; Poussigue, F.; Simon, A.-L.; Choi, C. M.; Knight, G.; Chirot, F.; MacAleese, L.; Antoine, R.; Dugourd, P. Conformational Changes in Amyloid-Beta (12–28) Alloforms Studied Using Action-FRET, IMS and Molecular Dynamics Simulations. *Chem. Sci.* **2015**, *6* (8), 5040–5047.

[20] Chan, W. C.; White, P. D. *Fmoc Solid Phase Peptide Synthesis : A Practical Approach*; Oxford University Press, 2000.

[21] Moore, B. N.; Blanksby, S. J.; Julian, R. R. Ion-Molecule Reactions Reveal Facile Radical Migration in Peptides. *Chem. Commun* **2009**, 5015–5017. https://doi.org/10.1039/b907833a.

[22] Maccarone, A. T.; Kirk, B. B.; Hansen, C. S.; Griffiths, T. M.; Olsen, S.; Trevitt, A. J.; Blanksby, S. J. Direct Observation of Photodissociation Products from Phenylperoxyl Radicals Isolated in the Gas Phase. *J. Am. Chem. Soc.* **2013**, *135* (24), 9010–9014. https://doi.org/10.1021/ja402610s.

[23] Lightfoot, P. .; Cox, R. .; Crowley, J. .; Destriau, M.; Hayman, G. .; Jenkin, M. .; Moortgat, G. .; Zabel, F. Organic Peroxy Radicals: Kinetics, Spectroscopy and Tropospheric Chemistry. *Atmos. Environ. Part A. Gen. Top.* **1992**, *26* (10), 1805–1961. https://doi.org/10.1016/0960-1686(92)90423-I.

[24] Ritz-Timme, S.; Collins, M. J. Racemization of Aspartic Acid in Human Proteins. *Ageing Research Reviews*. **2002**, *1* (1), 43–59. https://doi.org/10.1016/S0047-6374(01)00363-3.

[25] Pereverzev, A. Y.; Kopysov, V. N.; Boyarkin, O. V. Peptide Bond Ultraviolet Absorption Enables Vibrational Cold-Ion Spectroscopy of Nonaromatic Peptides. *J. Phys. Chem. Lett.* **2018**, *9* (18), 5262–5266.

[26] Ly, T., Zhang, X., Sun, Q., Moore, B., Tao, Y., & Julian, R. R. (2011). Rapid, quantitative, and site specific synthesis of biomolecular radicals from a simple photocaged precursor. *Chem. Comm.*, *47*(10), 2835.

[27] Hooi, M. Y. S.; Truscott, R. J. W. Racemisation and Human Cataract. D-Ser, D-Asp/Asn and d-Thr Are Higher in the Lifelong Proteins of Cataract Lenses than in Age-Matched Normal Lenses. *Age.* **2011**, *33* (2), 131–141. https://doi.org/10.1007/s11357-010-9171-7.

[28] Lebrilla, C. B. Ion-Molecule Reactions as Probes of Gas-Phase Structures of Peptides and Proteins. *Mass Spectrom. Rev.* **1997**, *16* (2), 53–71.

[29] Karanji, A. K.; Khakinejad, M.; Kondalaji, S. G.; Majuta, S. N.; Attanayake, K.; Valentine, S. J. Comparison of Peptide Ion Conformers Arising from Non-Helical and Helical Peptides Using Ion Mobility Spectrometry and Gas-Phase Hydrogen/Deuterium Exchange. *J. Am. Soc. Mass Spectrom.* **2018**, *29* (12), 2402–2412.

[30] Osburn, S.; Burgie, T.; Berden, G.; Oomens, J.; O'Hair, R. A. J.; Ryzhov, V. Structure and Reactivity of Homocysteine Radical Cation in the Gas Phase Studied by Ion–Molecule Reactions and Infrared Multiple Photon Dissociation. *J. Phys. Chem. A* **2013**, *117* (6), 1144–1150.

[31] Xia, Y.; Chrisman, P. A; Pitteri, S. J.; Erickson, D. E.; McLuckey, S. A. Ion/Molecule Reactions of Cation Radicals Formed from Protonated Polypeptides via Gas-Phase Ion/Ion Electron Transfer. *J. Am. Chem. Soc.* **2006**, *128* (36), 11792–11798.

[32] Moore, B. N.; Blanksby, S. J.; Julian, R. R. Ion–Molecule Reactions Reveal Facile Radical Migration in Peptides. *Chem. Commun.* **2009**, *33,* 5015-5017.

[33] Barlow, C. K.; Wright, A.; Easton, C. J.; O'Hair, R. A. J. Gas-Phase Ion-Molecule Reactions Using Regioselectively Generated Radical Cations to Model Oxidative Damage and Probe Radical Sites in Peptides. *Org. Biomol. Chem.* **2011**, *9* (10), 3733.

[34] Zhang, X.; Julian, R. R. Photoinitiated Intramolecular Diradical Cross-Linking of Polyproline Peptides in the Gas Phase. *Phys. Chem. Chem. Phys.* **2012**, *14* (47), 16243.

TOC